

Studies on toxicity of aluminum oxide (Al₂O₃) nanoparticles to microalgae species: *Scenedesmus* sp. and *Chlorella* sp.

I. Mohammed Sadiq · Sunandan Pakrashi ·
N. Chandrasekaran · Amitava Mukherjee

Received: 17 June 2010 / Accepted: 18 January 2011 / Published online: 4 February 2011
© Springer Science+Business Media B.V. 2011

Abstract In view of increasing commercial applications of metal oxide nanoparticles their toxicity assessment becomes important. Alumina (Al₂O₃) nanoparticles have wide range of applications in industrial as well as personal care products. In the absence of prior report on toxicological impact of alumina nanoparticles to microalgae, the principal objective of this study was to demonstrate the effect of the nanoparticles on microalgae isolated from aquatic environment (*Scenedesmus* sp. and *Chlorella* sp.). The growth inhibitory effect of alumina nanoparticles was observed for both the species (72 h EC₅₀ value, 45.4 mg/L for *Chlorella* sp.; 39.35 mg/L for *Scenedesmus* sp.). Bulk alumina also showed toxicity though to a lesser extent (72 h EC₅₀ value, 110.2 mg/L for *Chlorella* sp.; 100.4 mg/L for *Scenedesmus* sp.). A clear decrease in chlorophyll content was observed in the treated cells compared to the untreated ones, more effect being notable in the case of nanoparticles. Preliminary results based on FT-IR studies, optical and scanning electron microscopic images suggest interaction of the nanoparticles with the cell surface.

Keywords Nanoparticles · Alumina · Microalgae · EC₅₀ · Shading effect · Aggregates · Surface interactions · Health effects · EHS

Introduction

Metal oxide nanoparticles have been recently manufactured at the industrial level and have tremendous applications in water treatment, medicine, cosmetics, and engineering (Royal Society Publications 2004; USEPA 2005). For example, aluminum nanoparticles are already used in explosive combinations (Kaste and Rice 2004) and titanium dioxide nanoparticles are mostly used as a photocatalysts and adsorbents in consumer products like sunscreen lotion and as a catalyst in sterilization and chemical engineering (Fujishima et al. 2000; Meng et al. 2005; Pena et al. 2005). Since the applications of these engineered metal oxide nanoparticles increased in recent years, it is expected that metal oxide nanoparticles will find their way into the aquatic, terrestrial, and atmospheric environment, where their fate and behavior are largely unknown (Maynard et al. 2006; Nowack and Bucheli 2007). Recently we have studied the effect of aluminum oxide nanoparticles on *E. coli* (Sadiq et al. 2009). Toxicity effect of alumina (Al₂O₃) NP on bacteria was suggested to be due to the attachments of nanoparticles to bacterial cells (Jiang et al. 2009).

I. M. Sadiq · S. Pakrashi · N. Chandrasekaran ·
A. Mukherjee (✉)
Nanobio-Medicine Research Group,
School of Bio Sciences & Technology,
VIT-University, Vellore 632014, India
e-mail: amit.mookerjea@gmail.com

Algal toxicity tests are extensively applied to assess the effects of hazardous substances in water since; algae play an important role in the equilibrium of aquatic ecosystems, being the first level of the trophic chain to produce organics and oxygen. Modes of action of those particles with the biological organism are largely unknown though there were reports on toxicity to algae such as (*Pseudokirchneriella subcapitata* and *Desmodesmus subspicatus*) by titanium dioxide, zinc oxide, and copper oxide nanoparticles. However, to the best of our knowledge there are no studies till date dealing with alumina nanoparticles toxicity to algae.

The aim of the current investigation was to study the difference (if any) in toxic response of micron-sized and nanosized alumina particles toward microalgae isolated from aquatic environment.

Materials and methods

Chemicals

Dry alumina (Al_2O_3) NPs were procured from Sigma Aldrich (St. Louis, Missouri; CAS Number 1344-28-1). The supplier's data can be summarized as follows: gamma phase alumina nanopowder, particle size <50 nm. Bulk alumina powder was also procured from Sigma Aldrich (St. Louis, Missouri; Product Number H7881). The supplier's data can be summarized as follows: granular, particle size <5 μm .

Characterization of aluminum oxide nanoparticles

Scanning electron microscopic analysis (SEM)

The morphological features and particle size of the procured NPs were characterized by scanning electron microscopy. 10 mg/L of aluminum oxide nanoparticles were dispersed in Millipore water and sonicated for 15 min in 750 W (20 kHz) ultrasonic processor (Sonics Corp., USA). Aliquots of nanoparticles dispersion were placed in the cover slip and dried in hot air oven at 60 °C for 30 min; the slides were subjected to scanning electron microscopic analysis (FEI Sirion, Eindhoven, Netherlands).

Transmission electron microscopic analysis (TEM)

The particle size and shape of aluminum oxide particles were determined by TEM (Philips CM12 Transmission Electron Microscope, Netherlands). 10 mg/L of aluminum oxide nanoparticles was immersed in acetone solution after ultrasonic treatment for 5 min. The dispersed particles were then deposited onto the lacey-carbon-coated copper grid.

Powdered X-ray diffraction analysis

The crystal structures of the nanoparticles were characterized by powdered XRD (D8 Advanced X-ray diffractometer, Burker, Germany) scan with 2.2 kW Cu anode radiation at wavelength 1.54 Å produced by a Ceramic X-ray tube. About 250 mg of Al_2O_3 was deposited on the sample holder for scanning in the range 10°–100°. The crystalline formation was determined from the diffraction pattern and the crystallite size was calculated by the Scherrer formula.

Preparation of nanoparticles dispersion

The alumina NPs obtained from the suppliers were used to produce suspensions in OECD algal medium 201 (OECD 1984). Stock suspensions of nano and bulk alumina oxides were prepared in algal medium immediately before each experiment (3, 6, 12, 24, 48, 96, and 192 mg/L) in seven different concentrations and kept at 4 °C in refrigerator. Before use they were sonicated for 30 min in 750 W (20 kHz) ultrasonic processor (Sonics, USA).

Hydrodynamic size measurement

Dynamic light scattering also known as photon correlation spectroscopy was used to determine the hydrodynamic diameter of the particles in the suspensions. Diluted samples (40 mg/L) of alumina nanoparticles in suspension were used to determine the particle size. Samples were taken in two intervals (0 and 72 h). The measurements were conducted with the Zeta sizer (90 plus Particle Size Analyzer, Brookhaven instruments corporations, USA). The mean hydrodynamic diameter (z -average mean) was calculated from the autocorrelation function of the intensity of light scattered from the particles. The

software used was BI-DLSW control software for Windows in-built, supplied by the manufacturer (Brookhaven instruments corporations, USA).

Test organisms

The algal species (*Scenedesmus* sp. and *Chlorella* sp.) were isolated from VIT Lake, Vellore, India. Standard isolation protocol was followed for isolation of algal species as follows: Soil water mixture samples were collected in screw-capped bottles. Bold Basal Medium was used in this study and the initial pH value was 6.8. The media were autoclaved at 121 °C for 15 min before use. One gram mixture of soil and water sample was inoculated into 10 mL of the media in a large test tube and then cultured at 25 °C in a temperature-controlled incubator cum orbital shaker (I.L.E Co, India) for 3 weeks. Illumination was provided by white fluorescent light. The light intensity was 5000 Lux and the diurnal cycle was 12 h day/12 h night was maintained for 2 weeks. Algae culture was then flushed with sterile water and serial dilution was made and plated in BB medium for optioning pure cultures for 1 to 2 weeks. Genus level identification was done with the help of Centre for Advanced Studies (CAS) in Botany, University of Madras, India. The cultures were enriched with Modified Bold Basal Medium protocol (Fargasova 2001) for maintenance of the cultures throughout the study.

Algal growth inhibition study

Algal growth inhibition study was performed by using OECD test guidelines (OECD 1984). During 72 h growth experiments the exponential growth phase of algal cultures were used and exposed to various concentrations of the test substance under controlled conditions. It was insured that the cell concentration of the control culture (devoid of test substance) increased at least 16 times during 3 days. Also, the algal bio mass and total chlorophyll were measured at 24, 48, and 72 h intervals as described in previous reports (OECD 1984; Fargasova 2001). The algal growth inhibition was analyzed in batch cultures containing varying concentrations of alumina NPs and its bulk counterparts in suspensions (3, 6, 12, 24, 48, 96, and 192 mg/L).

Sterile side-arm Erlenmeyer flasks (250 mL) containing 50 mL of OECD medium with varied concentration of dispersed NPs (sonicated for 30 min to avoid aggregation) were inoculated with 1 mL of the freshly prepared algal suspension to maintain initial algal concentration of 10,000 cells/mL which was correlated with cell density as determined by cell counts in Neubauer hemocytometer (cells/mL). The flasks were then incubated for 72 h in a temperature controlled orbital rotary shaker (I.L.E Co, India) at (100 rpm) at 27 °C, illuminated with cool white fluorescent lights at a continuous light intensity of 5000 lux. High rotary shaking speed was selected to minimize aggregation and settlement of the NPs over the incubation period. Algal growth was measured as an increase in absorbance at 680 nm determined using a spectrophotometer (CL-157 colorimeter; ELICO Company, Hyderabad, India). The experiments also included a positive control (flask containing NPs and OECD medium, devoid of algal cells) and a negative control (flask containing algal cells and nutrient medium, devoid of NPs). The negative controls indicated the algal growth profile in the absence of NPs. The absorbance values for positive controls were subtracted from the experimental values (flasks containing OECD medium, algal inoculums, and NPs). Positive control OD values for different concentrations of nanoparticles in algal growth medium are given as follows: 3 mg/L (O.D: 0.01), 6 mg/L (O.D: 0.013), 12 mg/L (O.D: 0.02), 24 mg/L (O.D: 0.03), 48 mg/L (O.D: 0.04), 96 mg/L (O.D: 0.09), and 192 mg/L (O.D: 0.15). All the experiments were carried out in triplicate and the mean value was reported.

Optical microscopic analysis

Algal samples were collected at different time intervals such as initial 0 h and at the end of the experiment 72 h. Images were taken with Phase contrast microscope (Zeiss Axiostar Phase Contrast Microscope, USA). All images were taken in 50 µm scale to get a clear picture of the algal cells.

Scanning electron microscopic analysis

The surface of algal biomass after treating 48 mg/L of alumina nanoparticles were observed by scanning electron microscopy. Aliquots of algal cells

interacted with 48 mg/L of alumina nanoparticles were withdrawn during 72 h growth periods from the test system and a drop of algal sample was placed on cover slip and air dried. It was then chemically fixed for a period of 24–96 h using 4% (w/v) glutaraldehyde. Then the samples were rinsed in distilled water thrice and then dehydrated in graded series of ethanol (30, 50, 75, 85, 95, and 100%) for 3 min each and air dried under vacuum and kept in desiccators until use and then film was coated with gold and loaded for SEM analysis (Model S-3400 N, HITACHI).

FT-IR analysis

All cultivated algal strains (test as well as control) were prepared by an identical procedure for FT-IR spectroscopy. Two ml of the algal cell suspensions from 72 h test solution in presence of 40 mg/L alumina nanoparticles were harvested by centrifugation for 3 min at $14,000\times g$ at ambient temperature. The pellets were washed twice with 1 mL isotonic sodium chloride solution and centrifugations were repeated after which the pellets were dried for 30 min at 40 ± 0.5 °C in a hot air oven. The dried cells were subjected to Fourier transform-infrared (FT-IR) by potassium bromide technique in a Nicolet 6700 FT-IR Spectrometer (Thermo Scientific Instruments Groups, Madison, Wisconsin).

Statistical analysis

Algal growth inhibition tests with the green algae were performed in triplicates; the EC_{50} values (aluminum oxide concentration required to cause a 50% reduction in growth) were computed. The EC_{50} values were calculated using EPA probit analysis (program version 1.5). The level of significance was accepted at $P \leq 0.05$. In the figures, values are drawn as mean \pm standard error and in the table; EC and NOEC values are reported with mean value.

Results and discussion

Preliminary characterization

The preliminary characterization of aluminum oxide nanoparticles were carried out by High resolution SEM, TEM, and X-ray diffraction analyses before

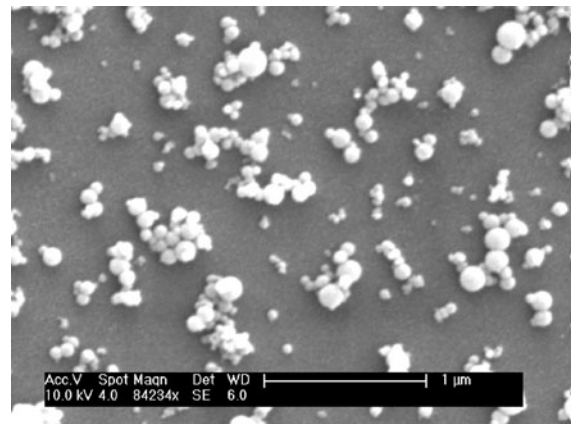


Fig. 1 Scanning electron micrograph showing procured aluminum oxide nanoparticles

introducing them to the test conditions. The high resolution SEM image of procured alumina nanoparticles is shown in (Fig. 1). Nearly spherical to spheroid shaped nanoparticles was observed. The particles were observed to be in agglomerated condition. The difference in primary size as given by the suppliers' data and experimentally obtained data may be due to aggregation of the nanoparticles in aqueous suspension. Further characterization regarding size and shape of the alumina nanoparticles were carried out by high resolution TEM images (Fig. 2). The TEM images taken in a 50 nm scale showed the alumina nanoparticles in different sizes ranging from 9 to 172 nm. Nearly all the particles exhibited spherical shape. Figure 3 shows the X-ray diffractograms of nano aluminum oxide. Six

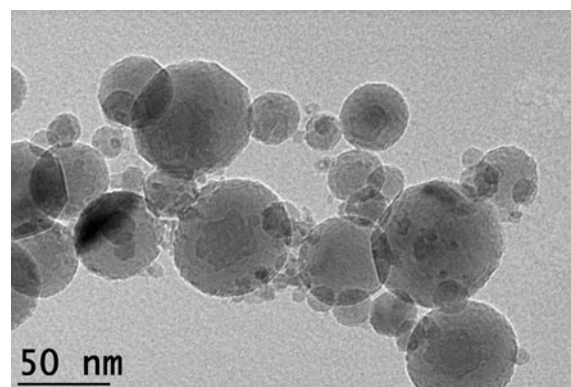
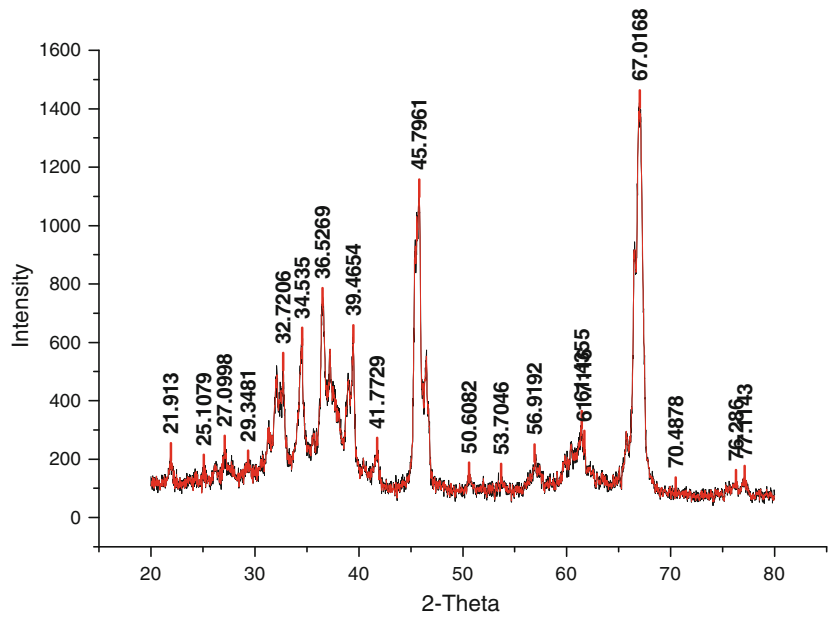


Fig. 2 TEM analysis of aluminum oxide nanoparticle dispersion

Fig. 3 Powdered XRD pattern of nano aluminum oxide



diffraction peaks (at 67.0°, 47.8°, 39.5°, 36.5°, 34.5°, 32.8°) were observed among them 67.01° and 47.8° were intense peaks. The data obtained were matched with the database of joint committee on Powder Diffraction Standards (JCPDS) card file No. 46-1215, which confirmed crystalline structure of alumina. The Debye-Scherrer equation was used to derive the crystallite size from the XRD data by determining the width of the 67.01° peak according to the equation. Where L is the particle size (nm), k is the Scherrer constant, β is the full width half maximum, θ is the half of Bragg angle, and λ is the wavelength of X-ray. The crystallite size was determined to be 17 ± 3 nm.

Hydrodynamic size analysis and aggregation state

The hydrodynamic particle size of nano as well as bulk alumina particle in the growth medium is shown in Table 1. Since we used the particles in suspensions for toxicological studies, it was of utmost importance to find out the size of the particles in test conditions

(secondary size), and the differences if any with the pristine size or primary size. Initial size of nano alumina immediately after ultra-sonication was found to be 172.1 nm and for bulk alumina it was 630.2 nm. We observed an increase size in both the cases with time. The mean particle size in growth medium devoid of test species was always less in comparison to that in test conditions for all the durations examined. Colloidal systems are dynamic non-equilibrium systems and are often sensitive to physical or chemical disturbances (Filella and Buffle 1993). Mixing under laboratory conditions that introduce shear forces are likely to perturb the dispersion state of ENPs, possibly leading to either further aggregation or to partial disruption of existing aggregation. The presence of algal species further complicates the situation. Therefore, the data presented in the Table 1 were average aggregation state of the particles with and without algal species in the growth medium. The average state in the control medium was solely dependent on surface chemistry of the particles and

Table 1 Hydrodynamic sizes of nano and bulk alumina particles in algal medium at different time intervals

Particles	Mean value of particle size at 0 h	Mean value of particle size at 24 h		Mean value of particle size at 48 h		Mean value of particle size at 72 h	
		Uninteracted	Interacted	Uninteracted	Interacted	Uninteracted	Interacted
Nano aluminum oxide (nm)	172.1	177.0	232.6	289.2	363.4	392.9	562
Bulk aluminum oxide (nm)	630.2	666.7	742.6	731.0	824.3	935.3	943

the solution parameters like pH and ionic strength (Handy et al. 2008).

Toxicity parameters

The important toxicity parameters such as EC₅₀, and NOEC are given in Table 2. As illustrated by the growth curves in Fig. 4a, b both bulk and nano forms of aluminum oxide were toxic to *Chlorella* sp. The 72 h EC₅₀ values for bulk alumina and nano alumina were 110.20 and 45.40 mg Al₂O₃/L, respectively. A typical concentration-dependent inhibitory effect of alumina was observed in both bulk and nano alumina particles with higher inhibitory response in the case of nanoparticles. Total chlorophyll content of *Chlorella* sp. treated with bulk and nano alumina particles were shown in Fig. 5a, b for the different concentrations of the particles used. In both the cases the total chlorophyll content was significantly lower in the treated cells compared to that of control cells. A concentration-dependent decrease in the chlorophyll content was noted, which confirmed growth inhibitory effect of increasing concentration of the particles. Comparing Fig. 5a, b enhanced toxicity effects of nanoparticles with respect to higher size bulk particles was evident.

Both bulk and nano form of aluminum oxide were also toxic to *Scenedesmus* sp. (Fig. 4c, d). The 72 h EC₅₀ values for bulk and nano alumina were 100.40 and 39.35 mg Al₂O₃/L, respectively (Table 2). A concentration-dependent decrease in total Chlorophyll content of *Scenedesmus* sp. was noted upon treating with bulk and nano alumina particles as shown in Fig. 5c, d.

Interaction of alumina particles with the microalgae and comparison between the test systems

Interaction of alumina particles with micro-algae were shown in culture flasks containing algal growth

medium, from left to right in Fig. 6a, d for *Scenedesmus* sp. and *Chlorella* sp. cultures, respectively: the first one is control flask devoid of nanoparticles the robust algal growth can be visualized. The remaining flasks contained with nanoparticles, which presumably inhibited the algal growth; most of the algal cells settled down at the bottom of these test flasks. The phase contrast microscopic images of the uninteracted algal cells are given in Fig. 6b, e for *Scenedesmus* sp. and *Chlorella* sp. cultures, respectively. Figure 6c, f depicts aggregates of particles covering almost all treated algal cells. Interestingly the flocculation of the algal cells was observed in the case of treated cells. The aggregation in the test solutions was already confirmed in the DLS studies.

A comparative analysis of growth data of the two test algal species treated with the bulk and nano form of Al₂O₃ revealed that *Scenedesmus* sp. were more sensitive than *Chlorella* sp. Alumina NPs were toxic to the both the tested algal species, while their bulk counterparts showed less toxicity, which could be due to the difference in particle size in suspension. The mean particle size in the test medium was found to be always more for bulk particles compared to the nanoparticles (Table 1). Their greater surface area per mass compared with larger-sized particles of the same chemistry, often enhances to a large extent the biological reactivity of the engineered nanoparticles (Oberdörster et al. 2005). This might result in catalysis of redox reactions upon contact with organic molecules (Zhang 2003) and also could have impact on photosynthetic or respiratory processes of algal species. Toxicity of TiO₂ ENPs to the green algae *Desmodesmus subspicatus* was shown to depend on the ENPs' specific surface area (Hund-Rinke and Simon 2006). Importantly, the mean particle size for nano alumina in the test medium was always greater than that in the growth medium without the test species (Table 1). This might be due to attachment of small aggregates of NPs on the surface of algae

Table 2 The toxicity of nano and bulk aluminum oxide to algae *Scenedesmus* sp. and *Chlorella* sp. (72 h growth inhibition)

Algae	EC ₅₀ ^a (mg/L) of nano Al ₂ O ₃	EC ₅₀ ^a (mg/L) of bulk Al ₂ O ₃	NOEC ^{a,b} of nano Al ₂ O ₃	NOEC ^{a,b} of bulk Al ₂ O ₃
<i>Scenedesmus</i> sp.	39.35	100.4	2.1	3
<i>Chlorella</i> sp.	45.40	110.20	1.8	3

^a Mean of three replicates

^b No-observed effect concentration

Fig. 4 a Growth inhibition effect of bulk aluminum oxide on *Chlorella* sp. cells. **b** Growth inhibition effect of nano aluminum oxide on *Chlorella* sp. cells. **c** Growth inhibition effect of bulk aluminum oxide on *Scenedesmus* sp. cells. **d** Growth inhibition effect of nano aluminum oxide on *Scenedesmus* sp. cells

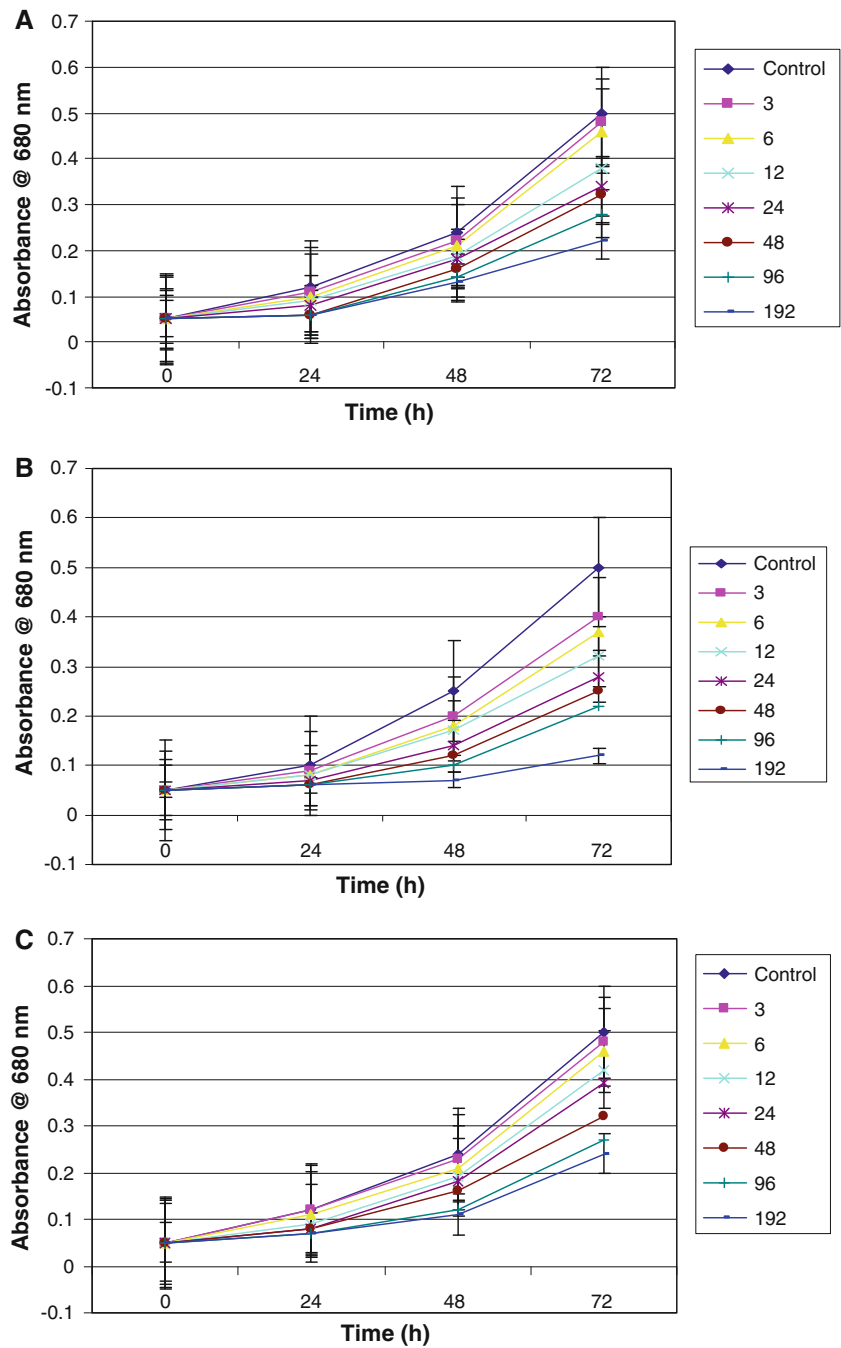
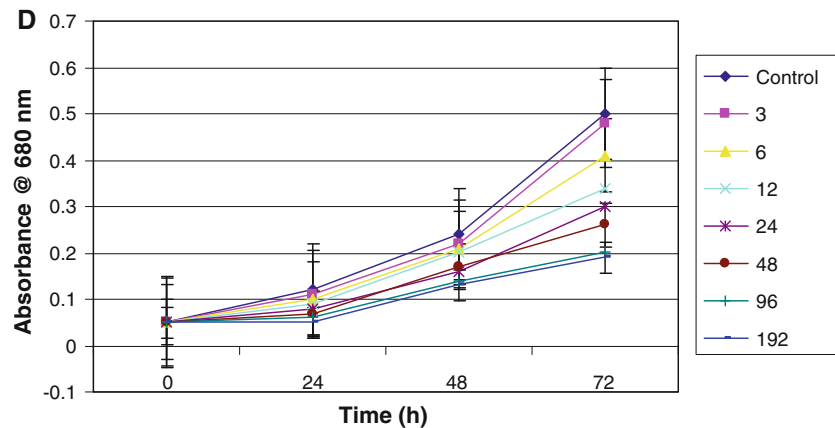


(Fig. 6c, f), though large aggregates were observed in NP suspensions.

In a study on toxicity of metallic alumina nanoparticles to the green algae *Pseudokirchneriella subcapitata* Griffitt et al. (2008) reported that the dissolution of nano alumina (1–4%) might be responsible for the toxic effect the but in our case

the dissolution of aluminum oxide was found to be beyond the detectable range (data not shown). However, our results corroborated with their study one important finding: different species behaved differently in susceptibility to nanoparticles and thus the EC₅₀ values were different among the species used in the experiments.

Fig. 4 continued



In this study we could not find detectable amount of Al^{3+} in the supernatant of the NP dispersion. This is due to insoluble nature of Al in near neutral region (Driscoll and Schecher, 1990). In a related study, Jiang et al. (2009) has also shown that from silica and alumina nanoparticles used in their study no detectable Al and Si were released. Therefore, the effect of soluble Al^{3+} was not considered for this study.

Sites of interaction

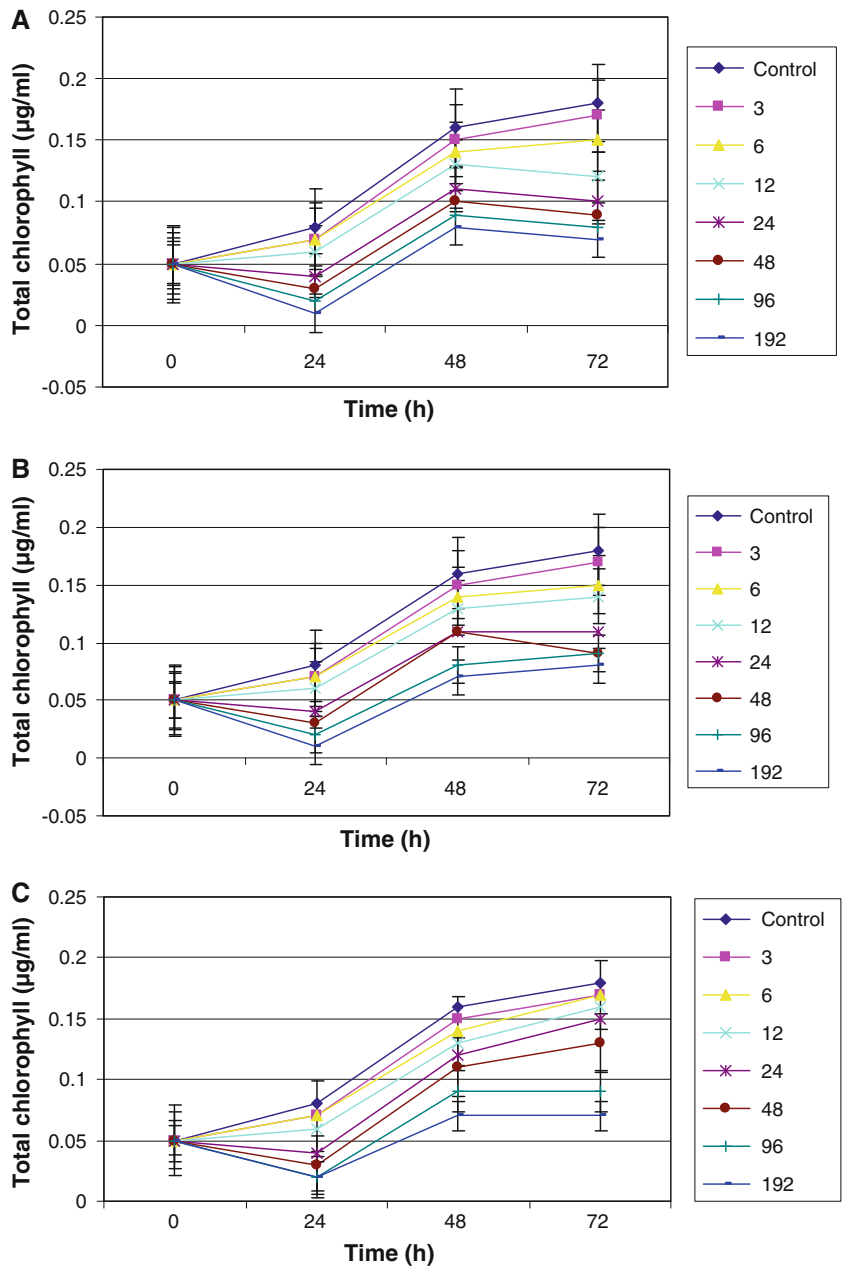
Most cells of plants, algae and fungi possess cell walls that constitute a primary site for interaction and a barrier for the entrance of ENPs into their cells. Major cell wall components are carbohydrates, linked to form a rigid complex network and proteins (Knox 1995). The functional groups such as carboxylate, phosphate, hydroxyl, amine, sulfhydryl, and imidazole present in these biomolecules offer a range of distinct active sites. Algae typically have glycoproteins and polysaccharides in their cell walls. To determine the active sites which possibly participated in interaction with the nanoparticles, FT-IR study of uninteracted and interacted algal cells was undertaken. Figure 7 shows the FT-IR spectra of interacted and control algal cells of *Chlorella* sp. in the mid infra red region ($4000\text{--}400\text{ cm}^{-1}$). The region $3700\text{--}3300\text{ cm}^{-1}$ is characteristic for O–H and N–H stretching vibrations (Guo and Zhang 2004). The region between 1800 and 1500 cm^{-1} shows characteristic bands for proteins, wherein $1700\text{--}1600\text{ cm}^{-1}$ is specific for amide-I bands (Dumas and Miller 2003) which is mainly due to C=O stretching vibrations of peptide bond signifying possible involvement of carboxyl group of COOH in

interaction with the nanoparticles. The regions from 1200 to 900 cm^{-1} are mainly dominated by a sequence of bands due to C–O, C–C, C–O–C, and C–O–P stretching vibrations of polysaccharides (Yee et al. 2004). These groups mainly occur in carbohydrates and cellular polysaccharides. Figure 8 shows the spectral details of *Scenedesmus* sp. cells. Even in this case distinct band shifts were noted. In this case also a band near 775 cm^{-1} revealed that a significant amount of alumina nanoparticles might be adsorbed by the cells.

Notably, in the alumina interacted cells for both the algae (Figs. 7, 8) we observed bands in $750\text{--}800\text{ cm}^{-1}$ region, which seems to be due to presence of alumina on the algal cell wall. A conspicuous band near 800 cm^{-1} has been reported in prior studies dealing with vibrational spectra of alumina. Tarte (1967) has shown the importance of the condensed or isolated state of the AlO_6 , and AlO_4 coordination groups present in $\gamma\text{-Al}_2\text{O}_3$ structure in order to define the characteristic infrared absorption band frequencies. Based on experimental results he demonstrated that for AlO_6 condensed octahedral and AlO_4 isolated tetrahedra, vibrational frequencies would be found in the range $680\text{--}500\text{ cm}^{-1}$, and $800\text{--}700\text{ cm}^{-1}$, respectively. Saniger (1995) also reiterated the significance of localized vibrations of the AlO_4 and AlO_6 coordination groups in $\gamma\text{-Al}_2\text{O}_3$ vibrational spectra. According to him the medium strong band near 753 cm^{-1} lies in the center of expected vibration range of isolated AlO_4 coordination groups. Similar results have also been supported by a few other researchers (Chandradass and Balasubramanian 2006; Naskar et al. 2002).

Summing up the spectral results, certain functional groups on the cell wall define the sites, which interact

Fig. 5 a Effect of bulk aluminum oxide on total chlorophyll content of *Chlorella* sp. cells. **b** Effect of nano aluminum oxide on total chlorophyll content of *Chlorella* sp. cells. **c** Effect of bulk aluminum oxide on total chlorophyll content of *Scenedesmus* sp. cells. **d** Effect of nano aluminum oxide on total chlorophyll content of *Scenedesmus* sp. cells



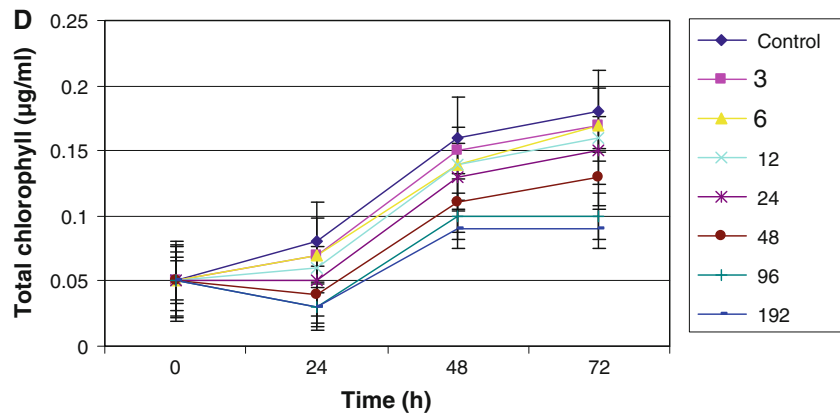
with the nanoparticles in the suspension. Therefore, we may conclude that the nanoparticles in suspension interacted with the algal cell wall (Surface Interaction).

Probable surface interactions

There are several physical–chemical factors like composition, concentration, size, ion dissolution

which play a major role in deciding toxic behavior of nanoparticles toward algae. The opacity of nanoparticles suspension can indirectly play a role in growth inhibitory effect by decreasing the light intensity. Navarro et al. (2008) have mentioned about physical restraint as one of the indirect mechanisms of nanoparticles toxicity toward algae. In their opinion, accumulation of nanoparticles on the algal surface causes a shading effect inhibiting

Fig. 5 continued



photosynthetic activity. Hoeckel et al. (2008) could not find any evidence for SiO₂ NPs (12.5 and 27 nm dia) uptake into the cells of *P. subcapitata* from electron microscopy images, but demonstrated that the particles were adsorbed onto the cell wall. Sorption of nanoparticles to the algal cell walls was reported to be a function of aggregation tendency and

interaction with other organics present in the system (Chen and Elimelech 2007). In another related study an increase in cellular weight was reported owing to TiO₂ nanoparticles adsorbed onto the algal surface (Huang et al. 2005).

In our study also Fig. 6c, f clearly demonstrated aggregates of alumina NPs around the algal cells. The

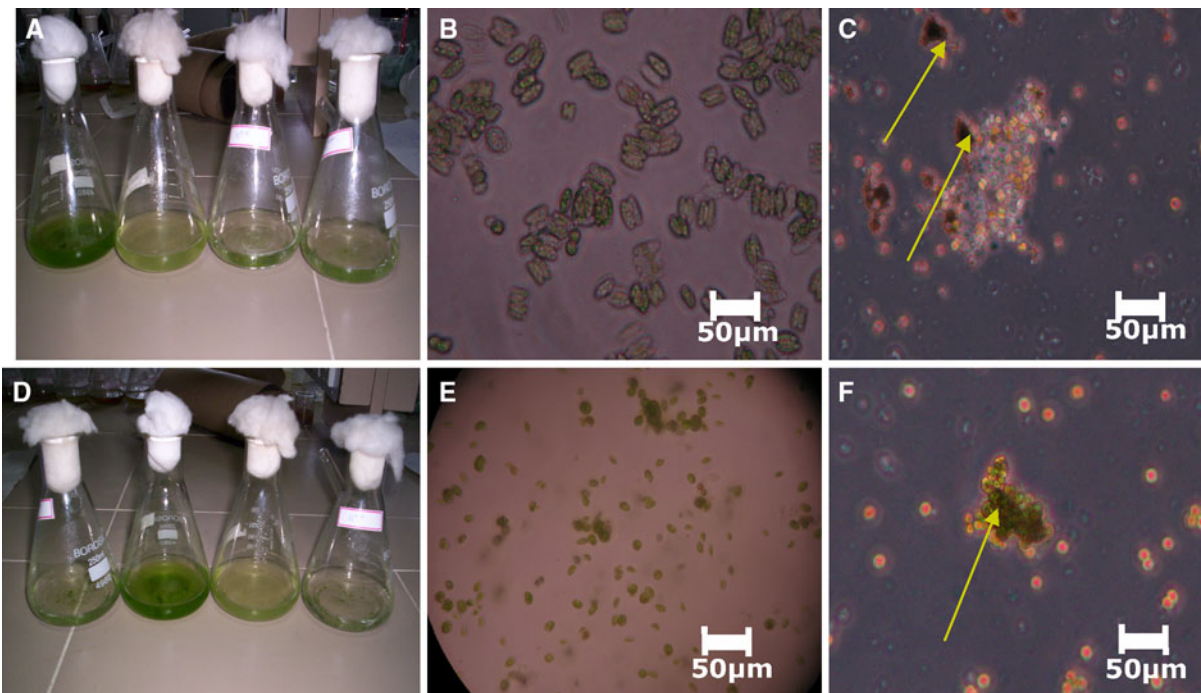


Fig. 6 **a** Culture media of *Scenedesmus* sp. interacted with alumina nanoparticles. **Arrow mark** indicating the algae settled at the bottom of the flask. **b** Phase contrast microscopic images showing morphology of uninteracted cells of *Scenedesmus* sp. **c** Phase contrast microscopic images showing agglomerates of nanoparticles clumped with algal cells of *Scenedesmus* sp. after interaction. **d** Culture media of *Chlorella* sp. Interacted with

alumina nanoparticles. **Arrow mark** indicating the algae settled at the bottom of the flask. **e** Phase contrast microscopic images showing morphology of uninteracted cells of *Chlorella* sp. **f** Phase contrast microscopic images showing agglomerates of nanoparticles clumped with algal cells of *Chlorella* sp. after interaction

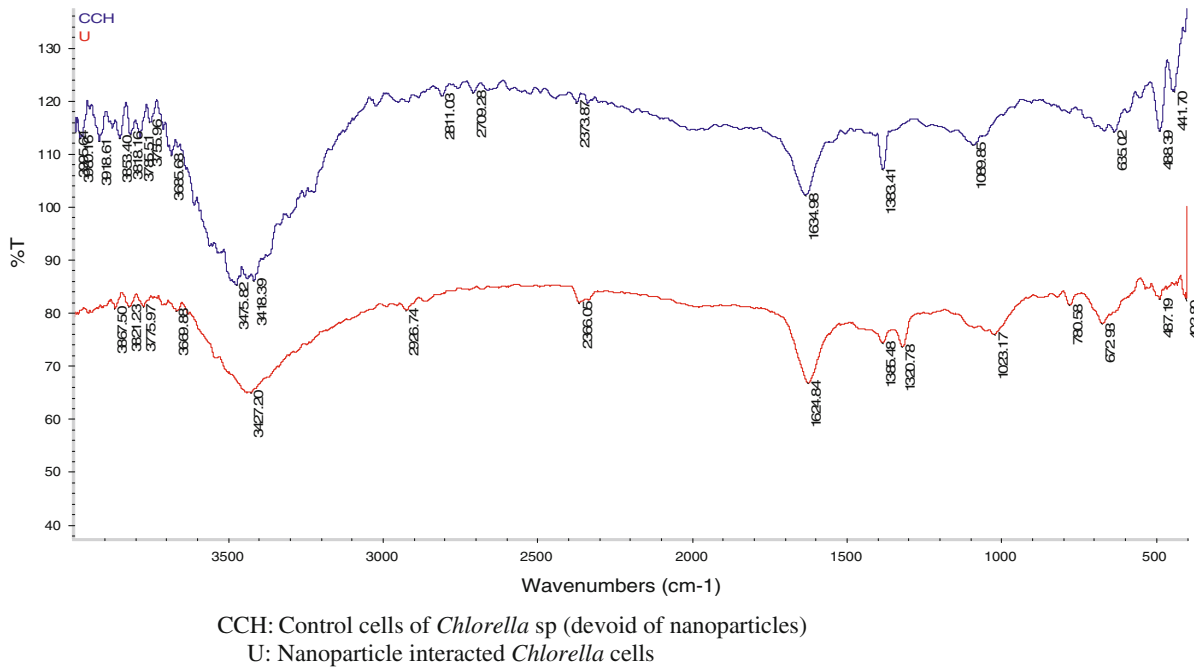


Fig. 7 FT-IR analysis of *Chlorella* sp. cells

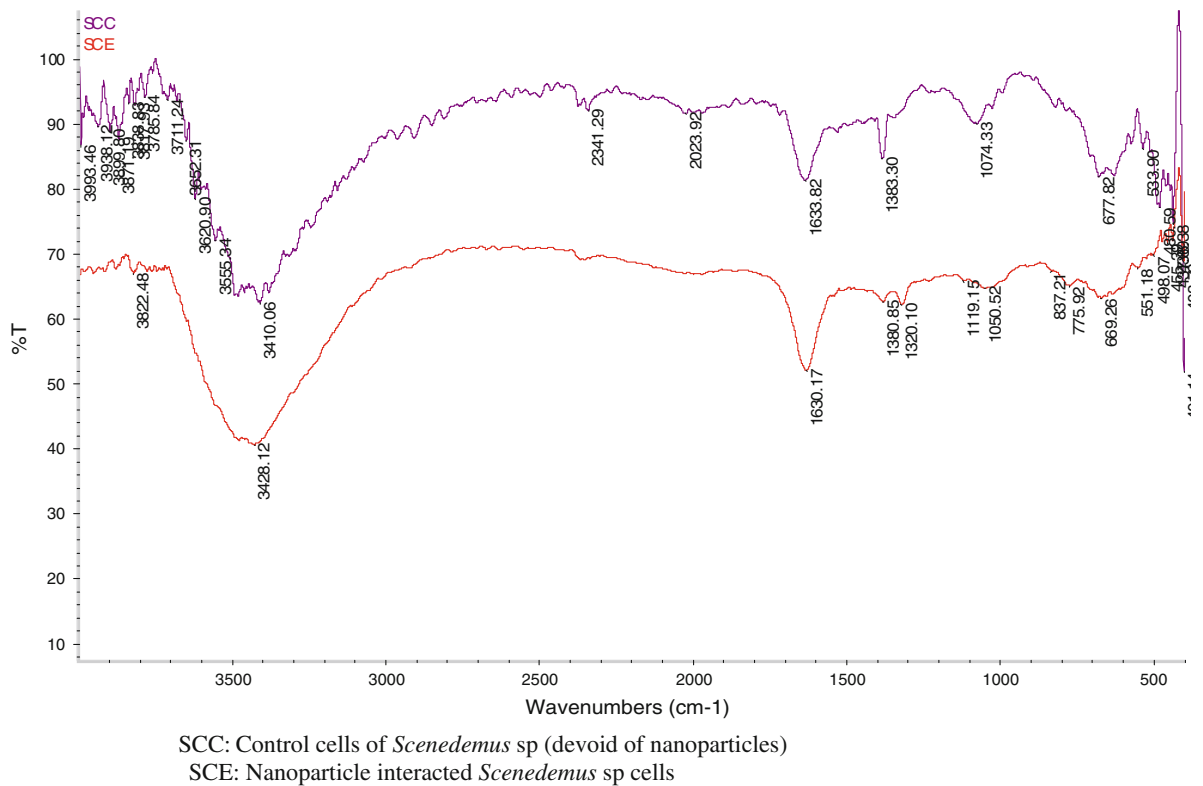


Fig. 8 FT-IR analysis of *Scenedesmus* sp. cells

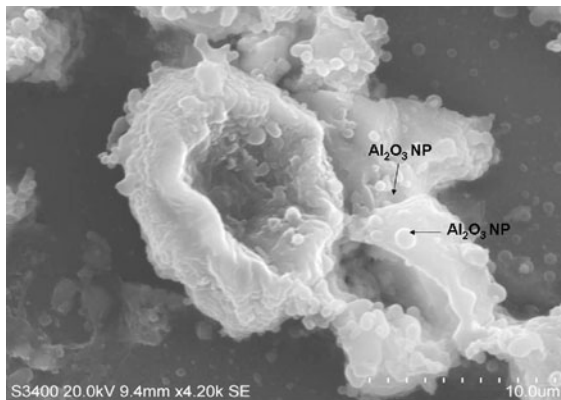


Fig. 9 Scanning electron micrograph showing attachment of aluminum oxide nanoparticles onto *Chlorella* cell wall after interaction

surface interaction was also confirmed from scanning electron micrograph (Fig. 9) showing the attachment of alumina nanoparticles onto the cell wall of chlorella sp. after the interaction. The FT-IR studies (Figs. 7, 8) also corroborated active participation of the surface groups in the interaction confirming further the case of adsorption of the aggregated NPs onto the surface. Decreased light availability (shading effect) owing to surface adsorption of the particles on the algal cell wall was one of the factors behind observed growth inhibitory effects. An increased surface area of the nano-sized particles compared to micron-sized particles would result in enhanced adsorption, thus causing more growth inhibitory effect (Fig. 4a–d). Further studies need to be undertaken to obtain detailed mechanistic understanding of the algal toxicity effects.

Conclusions

To our knowledge this is the first systematic study reporting the effects of alumina nanoparticles on algal growth. Alumina exhibited toxicity, both in bulk and nano form, though it was remarkably more toxic to algae as nanoparticles. Concentration-dependent decrease in the chlorophyll content may be due to the shading effect of alumina particles. The aggregation of the nanoparticles during test duration was confirmed through increase in hydrodynamic diameter. Algal species enhanced the aggregation

effect. The FT-IR studies with respect to the surface chemistry of the interacted cells demonstrate probable interaction between the particles and the surface active sites on the cell wall. The entrapment of algal cells in aggregates of alumina nanoparticles may play a pivotal role in toxicity to the algal specie.

References

- Chandradass J, Balasubramanian M (2006) Sol gel processing of alumina fibres. *J Mater Process Technol* 173:275–280
- Chen KL, Elimelech M (2007) Influence of humic acid on the aggregation kinetics of fullerene (C₆₀) nanoparticles in monovalent and divalent electrolyte solutions. *J Colloid Interface Sci* 309(1):126–134
- Driscoll CT, Schecher WD (1990) The chemistry of aluminium in the environment. *Environ Geochem Health* 12:28–48
- Dumas P, Miller L (2003) The use of synchrotron infrared microspectroscopy in biological and biomedical investigations. *Vib Spec* 32:3–21
- Fargasova A (2001) Interactive effect of manganese, molybdenum, nickel, copper I and II and vanadium on the freshwater alga *Scenedesmus quadricauda*. *Bull Environ Contam Toxicol* 67:688–695
- Filella M, Buffle J (1993) Factors controlling the stability of submicron colloids in natural waters. *Colloids Surf A: Physicochem Eng Aspects* 73:255–273
- Fujishima A, Rao TN, Tryk DA (2000) Titanium dioxide photocatalysis. *J Photochem Photobiol C* 1:1–21
- Griffitt RJ, Luo J, Gao J, Bonzongo JC, Barber DS (2008) Effects of particle composition and species on toxicity of metallic nanomaterials in aquatic organisms. *Environ Toxicol Chem* 27(9):1972–1978
- Guo J, Zhang X (2004) Metal-ion interactions with sugar. The crystal structure and FTIR study of an SrCl₂-fructose complex. *Carbohydr Res* 339:1421–1426
- Handy RD, Kammer FV, Lead JR, Hassellöv M, Owen R, Crane M (2008) The toxicology and chemistry of the manufactured nanoparticles. *Ecotoxicology* 17:287–314
- Hoeckel V, DeSchampelaere K, Vander Meer KAC, Lucas P, Janssen SCR (2008) The ecotoxicity of silica nanoparticles to the alga *Pseudokirchneriella subcapitata*: importance of surface area. *Environ Toxicol Chem* 27:127–136
- Huang CP, Cha DK, Ismat SS (2005) Progress report: short-term chronic toxicity of photocatalytic nanoparticles to bacteria, algae, and zooplankton. EPA Grant Number: R831721. <http://cfpub.epa.gov/ncer/abstracts/index.cfm/fuseaction/display.abstractDetail/abstract/7384/report/0>
- Hund-Rinke K, Simon M (2006) Ecotoxic effect of photocatalytic active nanoparticles (TiO₂) on algae and daphnids. *Environ Sci Pollut Res* 13:225–232
- Jiang W, Mashayekhi H, Xing B (2009) Bacterial toxicity comparison between nano- and micro-scale oxide particles. *Environ Pollut* 157:1619–1625
- Kaste PJ, Rice BM (2004) Novel energetic materials for the future force: the army pursues the next generation of propellant and explosives. *AMPTIAC Q* 8:84–90

- Knox JP (1995) The extracellular-matrix in higher-plants. 4. Developmentally- regulated proteoglycans and glycoproteins of the plant-cell surface. *J FASEB* 9:1004–1012
- Maynard AD, Aitken RJ, Butz T, Colvin V, Donaldson K, Oberdorster G, PhilLuria-bertani MA, Ryan J, Seaton A, Stone V, Tinkle SS, Tran L, Walker NJ, Warheit DB (2006) Safe handling of nanotechnology. *Nature* 444: 267–269
- Meng X, Dadachov M, Korfiatis GP, Christodoulatos C (2005) Methods of preparing a surface-activated titanium oxide product and of using same in water treatment processes. U.S. Patent Application Number 6,919,029
- Naskar MK, Chatterjee M, Lakshmi NS (2002) Sol-emulsion-gel synthesis of hollow mullite microspheres. *J Mater Sci* 37:343–348
- Navarro E, Baun A, Behra R, Hartmann NB, Filser J, Miao A, Quigg A, Santschi PH, Sigg L (2008) Environmental behavior and ecotoxicity of engineered nanoparticles to algae, plants, and fungi. *Ecotoxicology* 17:372–386
- Nowack B, Bucheli TD (2007) Occurrence, behavior and effects of nanoparticles in the environment. *Environ Pollut* 150:5–22
- Oberdörster G, Oberdörster E, Oberdörster J (2005) Nanotoxicology: an emerging discipline evolving from studies of ultrafine particles. *Environ Health Perspect* 113:823–839
- Organisation for Economic Cooperation and Development (1984) Algal growth inhibition test. OECD guidelines for testing of chemicals 201, Paris, France
- Pena ME, Korfiatis GP, Patel M, Lippincott L, Meng X (2005) Adsorption of As(V) and As(III) by nanocrystalline titanium dioxide. *Water Res* 39:2327–2337
- Sadiq MI, Chowdhury B, Chandrasekaran N, Mukherjee A (2009) Antimicrobial sensitivity of *Escherichia coli* to alumina nanoparticles. *Nanomed Nanotechnol Biol Med* 5:282–286
- Saniger JM (1995) Al-O infrared vibrational frequencies of γ - Al_2O_3 . *Mater Lett* 22:109–113
- Tarte P (1967) Infra-red spectra of inorganic aluminates and characteristic vibrational frequencies of AlO_4 tetrahedra and AlO_6 octahedra. *Spectrochim Acta* 23A:2127–2143
- The Royal Society & The Royal Academy of Engineering (2004) Nanoscience and nanotechnologies: opportunities and uncertainties. Royal Society Publications, London
- U.S. Environmental Protection Agency Nanotechnology White Paper (2005) http://www.epa.gov/osa/pdfs/EPA_nanotechnology_white_paper_external_review_draft_12-02-2005.pdf
- Yee N, Benning LG, Phoenix VR, Ferris FG (2004) Characterization of metal-Cyanobacteria sorption reactions: a combined Macroscopic and infrared spectroscopic investigation. *Environ Sci Technol* 38:775–782
- Zhang WX (2003) Nanoscale iron particles for environmental remediation: an overview. *J Nanopart Res* 5:323–332